Predicting the effects of sand erosion on collector surfaces in CSP plants

C.Sansom[a,*], P.Comley[a], P.King[a], H.Almond[a], C.Atkinson[a], E.Endaya[b]

[a]*Global CSP Laboratory, School of Applied Sciences, Cranfield University, MK43 0AL, UK*
[b]*Center for Solar Energy Research and Studies (CSERS), P.O Box 12932, Tripoli, Libya*

Abstract

This paper presents a methodology to predict the optical performance and physical topography of the glass collector surfaces of any given CSP plant in the presence of sand and dust storms, providing that local climate conditions are known and representative sand and dust particles samples are available. Using existing meteorological data for a defined CSP plant in Egypt, plus sand and dust samples from two desert locations in Libya, we describe how to derive air speed, duration, and sand concentrations to use within the Global CSP Laboratory sand erosion simulation rig at Cranfield University. This then allows us to predict the optical performance of parabolic trough collector glass after an extended period by the use of accelerated ageing. However the behavior of particles in sandstorms is complex and has prompted a theoretical analysis of sand particle dynamics which is also described in this paper.

1. Introduction

The performance of CSP plants is critically dependent on the quality of the solar field collectors or heliostats, characterized primarily by reflectivity and positional stability. To achieve high DNI the plants are often located in

---

* Corresponding author. Tel.: +44 1234 752955; fax: +44 1234 2946.
E-mail address: c.l.sansom@cranfield.ac.uk

desert regions where airborne sand and dust particles are an unwanted natural phenomenon. These particles settle on the collectors and heliostats to cause reflectivity losses, and in dust or sandstorm conditions can cause surface erosion. Washing and brushing is employed by solar plant operators to remove particles, a process that can lead to abrasion of the surface and permanent loss of optical reflectance. This work deals with the behavior of sand and dust particles in the vicinity of solar collectors and heliostats, and describes how to model the ageing of collector surfaces in the presence of airborne sand and dust particles.

2. Sand and dust particle characterization

MIL-STD-810G [1] makes it clear that dust and sand from a representative location is the preferred approach when simulating sand and dust erosion of collector and heliostat surfaces. Where that is not possible an alternative can be substituted. This can include red china clay and silica flour instead of dust and silica sand (at least 95% by weight SiO_2) instead of natural sand. Figure 1 shows that the MIL-STD silica compares favorably with real sand from
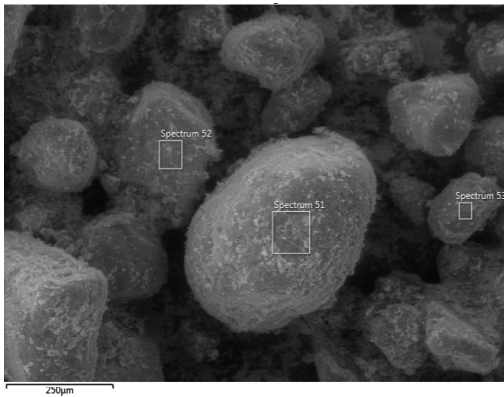

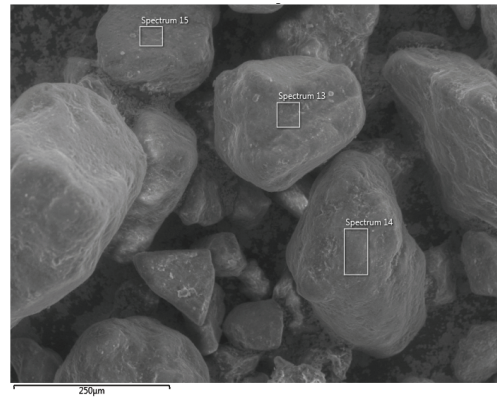Figure 1a: Mil-STD silica   Figure 1b: Libyan sand A

Tripoli in Libya from a dimensional standpoint, although the Libyan sand particles appear more angular. The hardness of Mil-STD silica is compared to Libyan sand 4 and 5 (both coastal sands) in Figure 2 below. Note the larger spread in hardness of the Libyan sand. The results are especially interesting when compared with the hardness of a collector glass from Ronda. As would be expected, the hardness of most of the sand and silica particles exceeds that of glass, but there is a significant quantity of sand or dust particles that are not as hard as the glass, making them
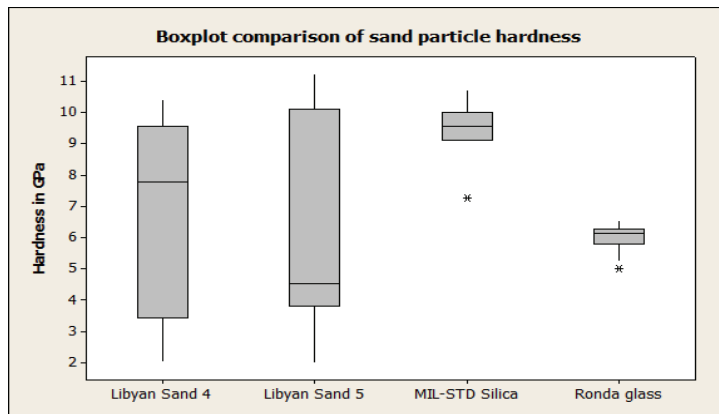

Figure 2: Hardness plots of various sands, and of Ronda manufactured glass

less likely to be a cause of surface erosion. It is not just in hardness where sands can vary. The elemental composition of sand particles can vary between locations. This can be important where chemical reactions are a significant cause of surface degradation. Figure 3 shows the analysis of elemental composition for both a Saharan
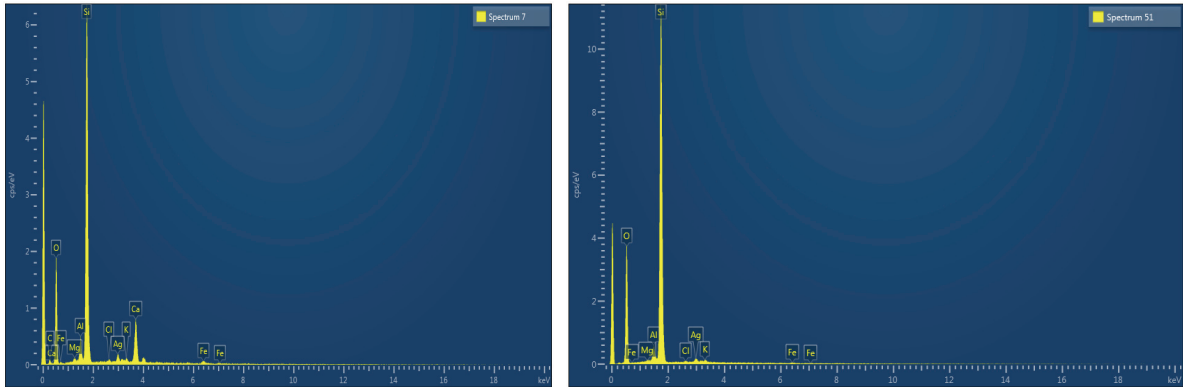

Figure 3: Compositional analysis (SEM plus EDX) for Libyan sand B (left) and MIL-STD sand (right) samples

sand (Libyan sand B) and the MIL-STD silica. The results, also summarized in Table 1 below, demonstrate the

Table 1 : Composition of MIL-STD silica (top) and Libyan Saharan sand (bottom)

Spectrum Label	C	O	F	Mg	Al	Si	Cl	K	Fe	Total
atomic %										
Spectrum 51		68.8		0.09	1.17	29.54	0.11	0.17	0.12	100
Spectrum 52	6.08	63.01			2.14	28.03	0.36		0.37	100
Spectrum 53		64.84	1.17		1.07	32.38	0.25	0.18	0.11	100
Spectrum 54	3.99	68.04	1.03		0.63	26.03	0.11	0.09	0.08	100
Spectrum 55		68.1			0.86	30.87	0.1	0.07		100
Spectrum 56	0.52	70.76	1.22		0.68	26.49	0.2	0.06	0.07	100

Spectrum Label	C	O	Na	Mg	Al	Si	S	Cl	K	Ca	Ti	Fe	Total
atomic %													
Spectrum 26	8.59	70.44		2.95	1.8	4.46		0.29	0.13	11.08		0.27	100
Spectrum 27	1.68	71.55		0.42	2.56	21.12		0.36	0.14	1.86		0.3	100
Spectrum 28	5.12	70.11		1.39	3.2	5.34	0.08	0.4	0.13	13.83		0.39	100
Spectrum 29	14.88	67.74	0.09	1.26	1.3	4.17	0.04	0.25	0.11	9.83	0.04	0.3	100
Spectrum 30		71.04	0.04	0.55	1.94	23.14	0.02	0.37	0.24	2.21	0.05	0.38	100
Spectrum 31	10.73	70.64	0.1	0.27	1.25	2.97		0.43	0.09	13.34		0.17	100

main difference between the desert sand and the MIL-STD silica to be the significant presence of calcium. The additional presence of sulphur, also missing from the MIL-STD silica suggests that the Libyan sand may contain small particles of gypsum (CaSO4 .2H2O) and bassanite (CaSO4 .0.5H2O). These particles originate in Iraq, and have been identified as airborne dust in middle eastern countries such as Kuwait [2]. Being finer in nature, they are more likely to adhere to glass and metal surfaces, as we discuss later.

3. Theoretical modelling of particles in sandstorms

3.1. Sand particle behavior (airborne)

The forces acting on a single sand particle are shown in Fig 4, where Fa is the force due to the air-flow (wind), Fg the particle weight under gravity, and Fe is the entrainment force caused by gusting, collisions, tunneling and vortices. The important fact to note is that the particle moves in the X-direction at less than the wind-speed [3].
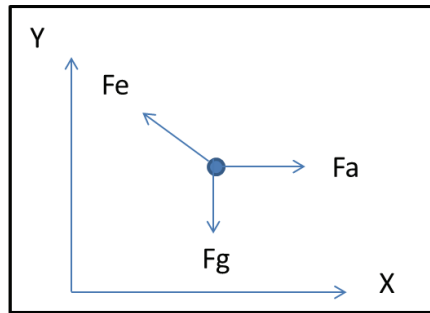
Figure 4: Forces acting on a single sand particle

For a single particle of diameter D_d and velocity u_d the entrainment force is given by equation (1),

$$F_e = C_D \pi \upsilon D_d (u_d - u) \qquad (1)$$

where CD is the coefficient of resistance and can be calculated form the Reynolds number, u is the wind velocity and υ is the air viscosity.

In order to determine the speed at which a given sand particle will impact a collector, it is necessary to consider the airflows around heliostats and parabolic troughs and the tilt angle of the collector. Given a streamline airflow at the first upwind collector, it can be shown that vortices are likely to be present for all downwind collectors, particularly at wind speeds of >15m/sec where sand erosion can occur [4]. In fact the drag and lift coefficients are independent of wind speed but are strongly influenced by the angle that any particle impacts the collector surface. Clearly the dynamic airflows will then depend on the layout of the solar field, and will be very dependent on local conditions. This analysis is beyond the scope of the current work, but is necessary for a full investigation of the airborne behavior of particles in sand storms.

3.2. Multi-particle sandstorm effects

The behavior of real particles in sandstorms is complex. It has been shown [5] that sand of 2.5μm and 10μm diameter becomes airborne in gusts of between 15-17m/sec. However, as explained in the previous section, the airborne sand particle will not achieve this velocity. According to the early work of Bagold [6] sand particles in the atmospheric aerosol within the range of 25-250μm in diameter will have a terminal velocity (also known as the Stokes velocity) of less than 10m/sec. A sand particle at rest on the ground can move in one of three ways, only one of which is of concern in the context of solar collector damage [7]. In surface creep the largest sand particles of between 500μm and 1mm in size are unable to obtain sufficient lift to overcome the gravitational force, and either roll or slide over each other. This is the classic case for desert dune sand and is the cause of the rounding of the sharp edges that often characterizes desert sand. Particles between 100-500μm tend to saltate, meaning that they do achieve sufficient lift to become airborne, but only for a short time and to an altitude of the order of centimeters. These particles may be a factor in the ageing of ground-based solar PV panels and of small ground-anchored heliostats, and will be the subject of future work. However for larger parabolic trough and heliostat fields it is only the third category of particles that are of concern, namely suspended particles. These particles, typically less than 100μm in size, become airborne with an acceleration proportional to the square of the difference between the wind speed and the particle speed. Also, this accelerating force is a function of the particle size, shape, and mass.

3.3. Sand and dust collisions with solar collectors

An airborne sand or dust particle that impinges on the surface of a solar collector can do one of four things. It can be reflected off the surface, it can stick to the surface, it can penetrate the surface, or it can react with the surface.In any of these cases the incident particle or the collector surface can be deformed as a result of the impact. According to Klikov at al [8], particles with Stokes velocities of around 10 m/sec should either stick to the surface or erode the surface, depending on particle size; with particles greater than 250μm causing erosion. Particles of the order of 250μm in size but with lower velocities are likely to rebound from the surface without causing damage. Particle adhesion is a consequence of a combination of forces. The smaller particles are of the order of 10-30μm, and can experience an attractive force of up to 100gms by virtue of elctrostatic and surface energy effects [9]. However the physical bonds can be much greater in the presence of condensed water vapour owing to capillary action, and strongest of all if the particle reacts with the surface to form chemical bonds. Although a sand particle and a glass surface may not react directly the condensed water molecules can dissolve soluble materials already present on the surface of the sand or the collector.Chemical bonds formed in this way can be extremely strong, and exceed the hardness of the glass.

In this paper we have concentrated our analysis on glass collectors, although it should be noted that dust will adhere better to plastic because of its electrostatic properties. Also of interest, a static mirror will collect four times more dust than a one-axis tracking mirror [10], and refractive concentrators are substantially less susceptible to soiling [11], since the light passes through the soiled region only once.

4.Sandstorm effects simulation: experimental results

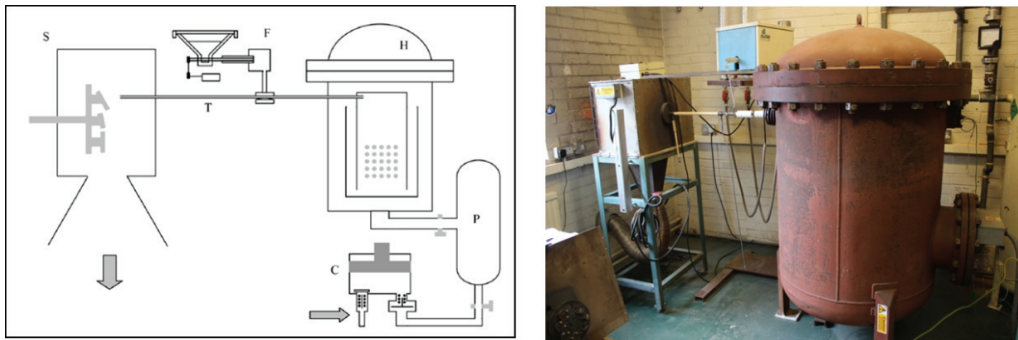Experiments were carried out in the Cranfield University "Erosion Rig", shown in Figure 5 below.

Figure 5: Sand erosion test equipment

The rig comprises a compressor (C) which supplies a pressure vessel (P), a pressurized heating system which forces air along a path before entering an acceleration tube. Sand particles are fed into this tube from a hopper (F) and through a venturi nozzle (T) and screw feeder into the sample chamber (S). The diameter of the nozzle is approximately 13mm.

For the work described in this paper, the impact angle was kept at 90°, based on the assumption of laminar flow as described earlier, and temperature at ambient in the range 20-22°C.

4.1. Climate data

Airborne particles of sand and/or dust are present in all locations of interest, and to varying degrees, as a natural consequence of climate conditions – one feature of which is sand and dust storms. For example, Table 2 below shows fallen dust in a number of regions of interest to solar plant planners.

Table 2: Fallen dust for various locations of interest to CSP plant stakeholders

Country	Location	Fallen dust tons/km^2/year	Reference
Iraq	Khur Al-Zubir	75.92	[12]
Iraq	Um Qasir	193.47	[13]
Oman	Al-Fahal	89	[14]
Saudi Arabia	Riyadh	392	[15]
Palestine	Dead Sea	45	[16]
Chad	North Dianena	142	[17]
Nigeria	Kano	137-181	[18]
Greece	Crete	10-100	[19]
USA	Arizona	54	[20]
USA	Nevada	4.3-15.7	[21]
USA	California	6.8-33.9	[21]
Libya	Libya	155	[22]
Morocco	Tan Tan	175	[23]
Morocco	Boujdour	219	[24]
Mauritania	Dakhla	191	[23]
Mali	Niger river	913-10446	[25]
Australia	Namoi valley	16.9-58.2	[26]
China	Shapotou	372	[27]

For an example of climate data we took 12 months meteorological data from Borg-El-Arab airport in Egypt, near to the site for the 5MWt MATS project CSP plant. The data includes average and peak wind-speeds and sandstorm frequency. Measurements in Borg-El-Arab in Egypt over a 24 month period produced an average wind speed of 5m/sec under normal conditions and 9.5m/sec during sandstorms. In the same time period in Borg-El-Arab there were 20 sandstorms per year, with an average duration of approximately 4 hours. As an example, an extract from the climate data for Borg-El-Arab for December 2010 showed high winds during the middle of the month, with a peak of 13m/sec (47km/hr) on December 12th.The duration of a sandstorm is approximate, given the difficulty in defining their presence, although the meteorological definition of a dust storm requires visibility of less than 1000m [28].

4.2. Sand erosion test equipment conditions

Using the climate data and sand particle evaluation results to calculate sand mass and air speeds, samples from a Ronda 1mm thick glass PT collector were tested in the sand erosion kit.

To illustrate the method for sandstorm simulation and the potential damage to solar collector surfaces, we chose to use Libyan sand and climate conditions from the Egyptian western desert (Borg-El-Arab airport). Ideally, climate conditions and sand that is representative of the location under investigation would be used, together with collectors of the type to be deployed at that location. Our decision to use Libyan sand, Egyptian climate data, and Ronda collector glass was driven by availability. However the experiments serve to illustrate the methodology.

As mentioned previously, the average wind speed during sandstorms in Borg-El-Arab was 9.5m/sec, and a rounded-up value of 10m/sec was used in our sand erosion rig. Since maximum gusts of between15-20m/sec were recorded we also investigated the effect of short exposures of collectors to sand velocities of around 17.5m/sec. A single sandstorm was simulated by the injection of 4g of sand at 10m/sec, equivalent to approximately 1 month of exposure in the Libyan Sahara/Egyptian Western deserts. Zhao et al [29] measured the sand flux and wind velocity in three areas of the Minqin region in China. One of these is a desert type environment. Wind speeds were measured at various heights, recording approximately 9 m/s at 1 m. This matches with the velocity observed in Borg-El-Arab and therefore characteristics of sand at this height should match that expected in Egypt. Through dust collection, a sand/dust concentration was measured at 1 m height of 104 mg/m3 in the desert region [29]. Assuming this value for the airborne concentration, moving at a velocity of 10 m/s implies the following

$$flux = concentration \times velocity \tag{2}$$
$$= 0.104 \; g/m^3 \times 10 \; m/s$$
$$= 1 \; g/m^2/s$$

The area of impact is a 20mm diameter circle.
$$impact \; area = \pi \times 0.01^2 \; m^2 \tag{3}$$
$$= 0.3 \times 10^{-3} \; m^2$$

Therefore the rate of sand impact should be
$$rate = flux \times area \tag{4}$$
$$= 1 \; g/m^2/s \times 0.3 \times 10^{-3} \; m^2$$
$$= 0.3 \; mg/s$$

Over one hour the mass of sand blown is therefore $0.3 \; mg/s \times 3600 \approx 1 \; g$.

This implies a mass of approximately 4g of sand for a typical sandstorm.

4.3. Evaluation of the sand erosion of glass collector surfaces

As the most significant effects are likely to be seen during sandstorm gusts, we initially evaluated potential for damage in the range around 13m/sec. Sand eroded collector pieces were examined for reflectance, and visually for chips and cracks. This data, shown in Figures 6 and 7 clearly shows a threshold around 17.5m/sec, above which erosion increases significantly, as measured by visual damage and by a reduction in surface reflectance.

This demonstrates the need to place collectors in the "stow" position during the worst sand storms, particularly when wind speeds are greater than 15m/sec. However, we need to remember that the sand particle terminal velocity will be less than the wind speed, and stowing of the collectors is a precautionary measure. In Figures 6 and 7, sand A is Libyan city sand (generally with smaller particle size and more irregular in shape) and sand B is Saharan sand (generally with larger particle size and with rounded edges, a consequence of rolling dune sand). The larger particles in sand B have a higher kinetic energy and cause more damage (Figure 6), whereas the smaller particles in sand A adhere to the surface extremely well at higher wind speeds, whereas larger particle can reflect (or bounce), as shown in Figure 7.

In order to simulate sand storm effects over time, in our case a speed of 10m/sec was chosen, as explained earlier. This is location dependent, as indeed is the mass of sand used in the experiment (4g per sandstorm in our case).
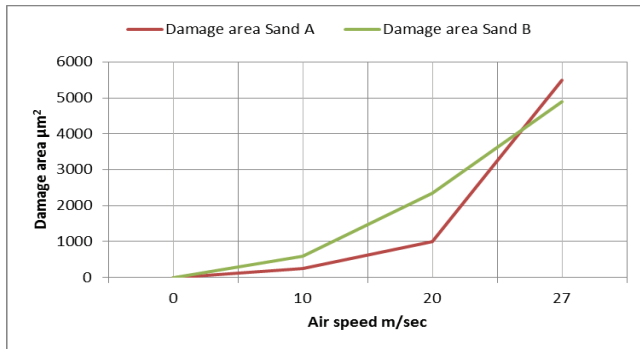

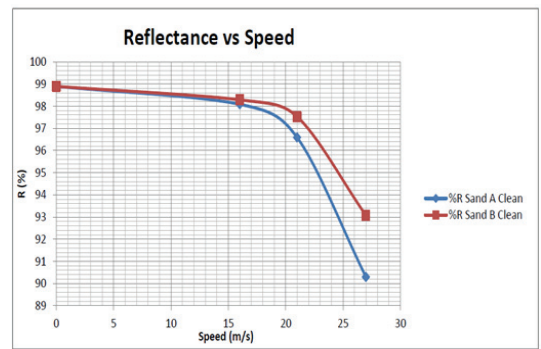Figure 6 : Sand-induced visual damage of glass

Figure 7 : Glass reflectance after sand erosion

The results for the simulation of a single sandstorm are shown in Figure 8 below, using 4g of three different sand particle types (Libyan sand 4, Libyan sand 5, and MIL-STD silica).
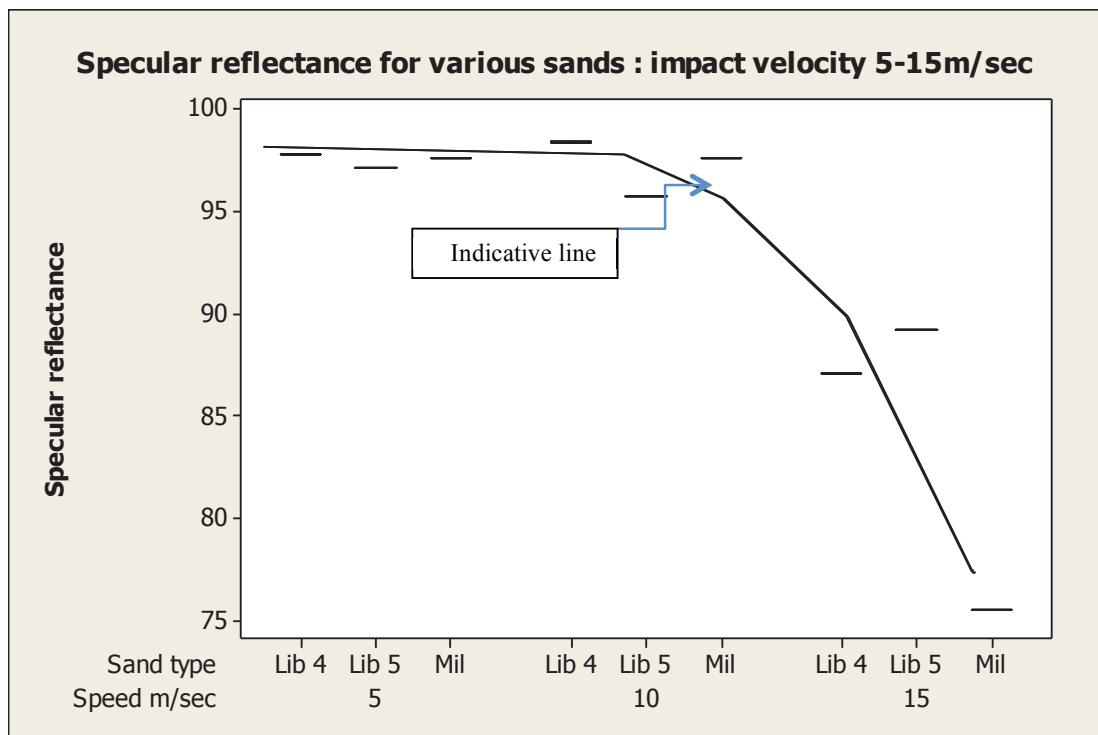

Figure 8: Sandstorm simulation for 3 types of sand

Measurements of specular reflectance show that there is little or no effect from all sand types at the sandstorm simulating velocity of 10m/sec. Once again, there is a loss of reflectance at speeds of the order of 15m/sec. However, visual inspection of the surface, an example of which is shown in Figure 9, suggests that this loss in reflectance is due to small particles of sand adhering to the surface of the glass and is not evidence of damage.
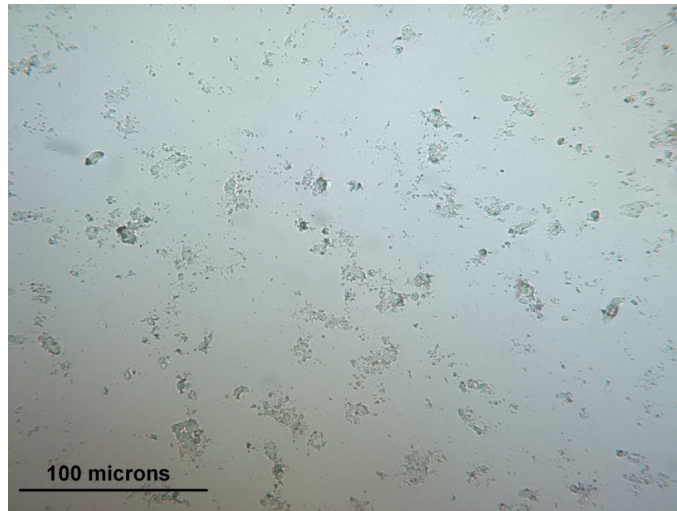

Figure 9: Libyan sand 5 showing sand adhesion after 4g deposition at 15m/sec

5.Conclusions

Using existing meteorological data from a representative CSP plant location plus sand and dust samples from two appropriate desert locations we describe how to derive air speed, duration, and sand concentrations to use within a laboratory based sand erosion simulation rig to predict the optical performance of parabolic trough collector glass after a prolonged period in an arid region prone to sand and dust storms. The impact on surface reflectance, roughness, and visual quality is presented. The method can be adapted for any arid location, given that climate data and sand samples can be obtained.

References

[1] MIL-STD-810G, accessed online at http://assist.daps.dla.mil/quicksearch/
[2] J. Al-Awadhi, Kuwait Journal of Science and Engineering, 32, 135-152 (2005)
[3] S.Lui et al, Computer Animation and Virtual Worlds, 18, 259-269 (2007)
[4] F.Christo, Renewable Energy, 39, 356-366, (2012)
[5] J. Lee et al, Geomorphology, 105, 18-27 (2009)
[6] R. Bagnold, The physics of blown sand and desert dust, Methuen and Co. Ltd. London (1965)
[7] J.Travis, Atmospheric-Surface exchange of particulate and gaseous pollutants, 907-9, Proceedings of Symposium held at Richland, Washington, USA (1974)
[8] S. Klinkov et al, Aerospace Science and Technology, 9, 582-591 (2005)
[9] R. Berg, Heliostat Dust Buildup and Cleaning Studies, Sandia Laboratories (1978)
[10] S. Biryukov et al, Solar Energy, 66, 371-8 (1999)
[11] M. Garcia, Doctorate Thesis, Institute de Energia Solar (2009)
[12] F. Khalaf et al, Kuwait Institute for Scientific Research, Final Report No. KISR/PPI 108/EES-RF-8016 (1980)
[13] I. Gharib et al, Kuwait Institute for Scientific Research, Final Report No. KISR/ 2266 (1987)
[14] M. Badawy et al, Bulletin of Environmental Contamination and toxicology, 49, 813-820 (1992)
[15] A. Modaihsh, Journal of Arid Environments, 36, 211-223 (1997)
[16] A. Singer et al, Journal of Arid Environments, 53, 41-51 (2003)
[17] J. Maley, Quaternary Research, 18, 1-16 (1982)

[18] G.McTainsh et al, Geomorphologie, 26, 417-435 (1982)
[19] K. Pye, Earth Surface Processes and Landforms, 17, 271-288 (1992)
[20] T. Péwé, Geological Society of America, Special. Paper 186:1-10 (1981)
[21] M. Reheis, Journal of Arid Environments, 67, 487-520 (2006)
[22] S. O'Hara et al, Atmospheric Environment, 40, 3881-3897 (2006)
[23] C. Rott, MSc dissertation, Royal Holloway University of London (2001)
[24] F. Khiri et al, Journal of African Earth Sciences, 39, 459-464 (2004)
[25] G. McTainsh et al, Catena, 29, 307-322 (1997)
[26] S. Cattle et al, Catena, 47, 245-264 (2002)
[27] X. Li et al, Restoration Ecology, 12, 376-390 (2004)
[28] A.Al-Kulaib, Climate of Arabian Gulf, That Alsalasil Press, Kuwait p87 (1990)
[29] M. Zhao etal, Science China Earth Sciences, 54, 703-710 (2011)

Predicting the effects of sand erosion on collector surfaces in CSP plants

Sansom, Christopher L.

2015-06-05